Bioorganic & Medicinal Chemistry 20 (2012) 2803–2810

Contents lists available at SciVerse ScienceDirect

Bioorganic & Medicinal Chemistry

journal homepage: www.elsevier.com/locate/bmc

Synthesis and fungicidal activity of tubulin polymerisation promoters. Part 2: Pyridazines

Clemens Lamberth *, Stephan Trah, Sebastian Wendeborn, Raphael Dumeunier, Mikael Courbot, Jeremy Godwin, Peter Schneiter

Syngenta Crop Protection AG, Crop Protection Research, Schaffhauserstr. 101, CH-4332 Stein, Switzerland

ARTICLE INFO

Article history:
Received 29 November 2011
Revised 12 March 2012
Accepted 15 March 2012
Available online 24 March 2012

Keywords:
Tubulin
Pyridazine
Heterocycle
Fungicide
Crop protection

ABSTRACT

Special tetrasubstituted pyridazines are potent fungicides by promoting the tubulin polymerisation, hereby disrupting the microtubule dynamics in the fungus. They are monocyclic analogs of similar substituted triazolopyrimidines and pyridopyrazines with the same mode of action. The fungicidal activity of these pyridazines was evaluated against the plant pathogens *Botrytis cinerea* (grey mould), *Mycosphaerella graminicola* (wheat leaf blotch) and *Alternaria solani* (potato and tomato early blight). Structure–activity relationship studies revealed the importance of a methyl and a chlorine substituent next to both ring nitrogen atoms and two aryl or heteroaryl groups in the other two pyridazine positions.

1. Introduction

Microtubules are hollow cylindrical tubes found in all eukaryotic cell types. These essential cytoskeletal protein polymers play a pivotal role in maintaining the growth, shape, division, motility and functioning of the cell. Microtubules are key components of the mitotic spindle, which enables the segregation of chromosomes during the process of mitosis. They are built by polymerisation of two closely related heterodimers composed of α- and β-tubulin subunits. Interference with the microtubule homeostasis by disrupting the dynamic equilibrium between the assembly of tubulin into microtubules or, inversely, the depolymersiation of microtubules into tubulin leads to arrested cell division and consequently to apoptosis. Compounds which are able to inhibit one of these two important processes are called antimitotics.[2]

Antimitotic drugs are a well-established class of chemotherapeutic anti-cancer agents, as demonstrated by the two naturally occurring tubulin polymerisation promoting families of taxanes, for example, paclitaxel and docetaxel, and vinca alkaloids, such as vinblastine and vincristine.[3–9]

In the meantime, compounds with this mode of action attract more and more attention for their fungicidal efficacy. Antimitotics are used already as agrochemical fungicides, such as the amides zoxamide[10,11] and ethaboxam,[12,13] as well as the benzimidazoles benomyl,[14,15] carbendazim,[14] thiabendazole[15,16] and fuberidazole,[15] most of them being inhibitors of the tubulin polymerisation. However, promotion of tubulin polymerisation would still be a novel mode of action on the fungicide market.

[1,2,4]Triazolo[1,5-*a*]pyrimidines, such as BAS600F (**1**),[17] have been identified as promotores of tubulin polymerisation. This class of experimental fungicides, which has been discovered by Shell in the early 1990s,[18] is highly active against a broad range of different plant diseases.[19] In addition, some [1,2,4]triazolo[1,5-*a*]pyrimidine mimics, in which the five-membered triazole ring is replaced by a six-membered heterocycle, have also been described. Such pyrido[2,3-*b*]pyrazines,[1] for example, **2**, and pyrido[3,2-*e*][1,2,4]triazines,[20] such as **3**, display a similar efficacy against phytopathogens as the related triazolopyrimidines. Recently Sumitomo discovered, that pyridazines, such as **4**, are suitable monocyclic analogs of the before mentioned bicylic tubulin polymerisation promoters.[21] This is not by surprise, because also in medicinal chemistry, pyridazines have been able to mimic similar substituted bicyclic imidazopyrimidine and imidazotriazine $GABA_A$ agonists.[22] Actually it is a closely related substitution pattern, which is common to those 5,6-bicylic, 6,6-bicyclic and monocyclic promoters of tubulin polymerisation shown in Figure 1. They all carry adjacent to a ring nitrogen atom a halogen substituent, next to it there is a 2,4,6-trifluorophenyl ring, which is followed by either an amine or another phenyl group. In the case of the heterobicyclic tubulin promoting fungicides, the second ring which is annelated between the amino substituent and a ring nitrogen of the persubstituted ring, is generally unsubstituted.

The pyridazine ring has a long-standing history as part of biologically active compounds. Several highly efficacious pharmaceu-

* Corresponding author. Tel.: +41 62 8660224; fax: +41 62 8660860.
E-mail address: clemens.lamberth@syngenta.com (C. Lamberth).

0968-0896/$ - see front matter © 2012 Elsevier Ltd. All rights reserved.
http://dx.doi.org/10.1016/j.bmc.2012.03.035

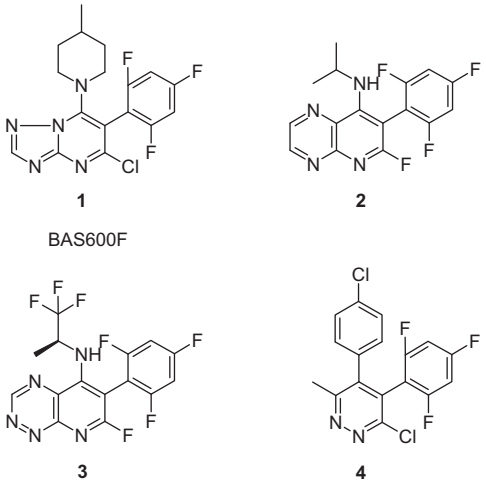

Figure 1. Different mono- and bi-heterocyclic fungicidally active tubulin polymerisation promoters.

ticals[23,24] and agrochemicals[25–27] bear a pyridazine scaffold. Outside of the relatively narrow patent claims of Sumitomo covering **4**, we have prepared many different pyridazines, for example, derivatives of **4** with a fluorine or a cyano instead of the chloro substituent in position 3,[28] with a heteroaryl ring instead of the trifluorophenyl in position 4,[29] with a heteroaryl[30] or an alkyl[31] group instead of the 4-chlorophenyl in position 5, and with a halogen or an alkoxy group instead of the methyl group in position 6.[32] In this article, we describe the synthesis and structure–activity relationship of these fungicidal pyridazine tubulin polymerisation promoters.

2. Results and discussion

2.1. Chemistry

Most of those diversely substituted pyridazines have been prepared according to the original procedure, which researchers at Sumitomo have used to approach such tetrasubstituted pyridazines. This efficient process is demonstrated in Scheme 1 for the synthesis of the chlorothienyl derivative **10**. The key step of this route is the cyclocondensation of the α-bromoketone **7**, which is available in two steps from 5-chlorothiophenecarboxylic acid (**5**) via the Weinreb amide **6**, with 2,4,6-trifluorophenylacetic acid to the hydroxyfuranone **8**. This unique one-pot ring closure reaction proceeeds via three different partial steps, which will be further explained in Scheme 2.[33,34] The subsequent ring enlargement of the methyl- and hydroxy-substituted butenolide **8** to the pyridazinone **9** has first been described by Caspi and Piatek.[35,36] Finally **9** is converted by chlorination to the fungicidally active pyridazine **10**.

As worked out by researchers at Merck,[33] the one-pot preparation of the hydroxyfuranone **8** starts with the substitution of the bromine in **7** by the triethylammonium salt of 2,4,6-trifluorphenylacetic acid to provide the ester **11**, which after addition of DBU undergoes an intramolecular aldol condensation to the furanone **12**. Finally, bubbling air through the reaction mixture results in oxidation to the desired hydroxyfuranone **8**.

Using the general synthesis shown in Scheme 1, the pyridazine substituents in positions 4, 5 and 6 can be easily varied by application of different ketones and carboxyclic acids. Also several different substituents can be introduced in position 3 by replacement of the chloro function. The only limitation of this method is the fact, that it is not possible to exchange the typical methyl group in position 6 by non-carbon linked substituents, such as halogen, alkoxy, amino etc. Because we wanted to test also such substituents in pyridazine position 6, we envisaged a maleic anhydride instead of the typically used methylfuranone as five-membered ring intermediate. Therefore we started from the 4-chlorophenylglyoxylic acid **14**, which is available in two steps from chlorobenzene (**13**) via Friedel–Crafts acylation and saponification (Scheme 3). After transformation of **14** into its potassium salt, a Perkin-type condensation[37] with 2,4,6-trifluorophenylacetic acid delivered the diarylmaleic anhydride **15**. This sensitive intermediate could be transformed with hydrazine hydrate to the pyridazinedione **16**, which after dichlorination delivered the 3,6-dichloro-4,6-diarylpyridazine **17**. This compound is not only a close analog of Sumitomo's pyridazine **4**, but also a versatile building block for further transformations. Its conversion with one equivalent of sodium methoxide led regioselectively to **18**, obviously because of sterical hindrance in the attack of the other chloro group by the two *ortho*-fluoro substituents in the adjacent phenyl ring. In a similar manner, also the regioselective introduction of thioalkyl, different amino groups and other halogens, such as fluoro and iodo into pyridazine position 6 is possible.

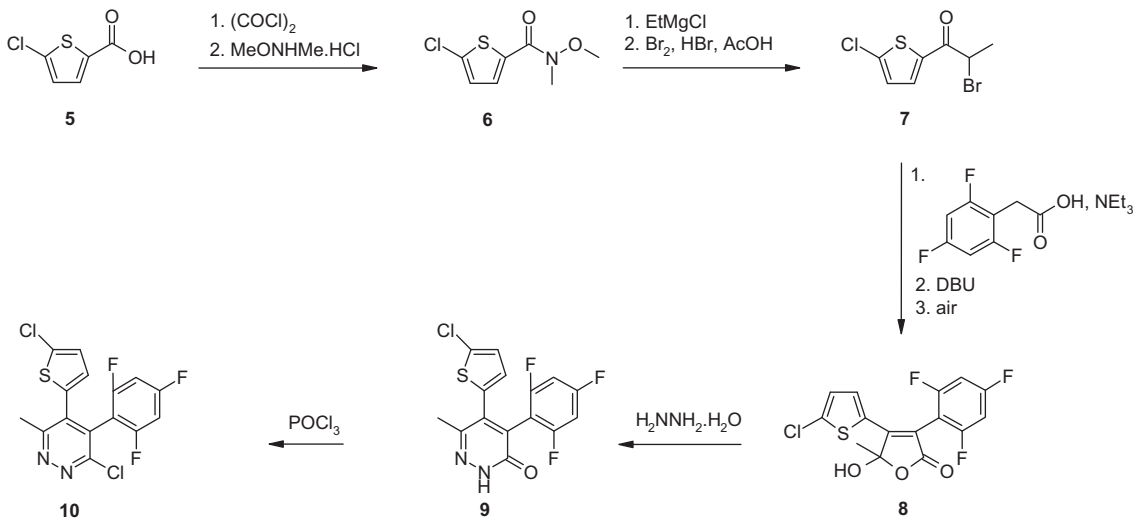

Scheme 1. General synthesis of pyridazine fungicides at the example of **10**.

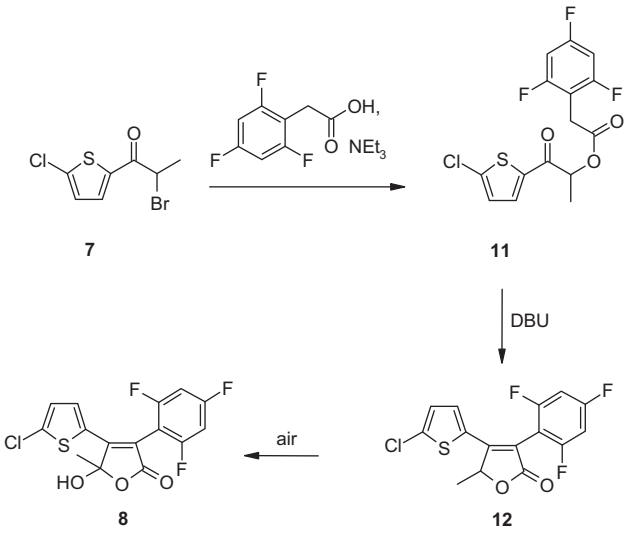

Scheme 2. One-pot cyclocondensation of the hydroxyfuranone **8** from the α-bromoketone **7** and 2,4,6-trifluorophenylacetic acid.

2.2. Mode of action

The highly active pyridazine fungicide **10** was submitted to a polymerisation assay on pure porcine tubulin to check if also these monocyclic compounds, as already confirmed for the mentioned bicyclic subclasses, are disrupters of the microtubule dynamics. It was compared against paclitaxel, which is a known tubulin polymerisation promoter and for which in the two highest concentrations a clear increase in the OD_{340} value could be detected. A very similar pattern was observed for **10**, indicating a similar effect on tubulin polymerization to paclitaxel. However, little effect of **10** has been observed at lower concentrations, which indicates a lower promoting effect of this compound on pure porcine tubulin compared to paclitaxel (Fig. 2).

2.3. Structure–activity relationships

Tetrasubstituted pyridazine fungicides, such as **10** and **18**, bear four completely different functional groups. A thorough structure–activity relationship study of these positions revealed, that each substituent exerts a distinct influence on the fungicidal efficacy.

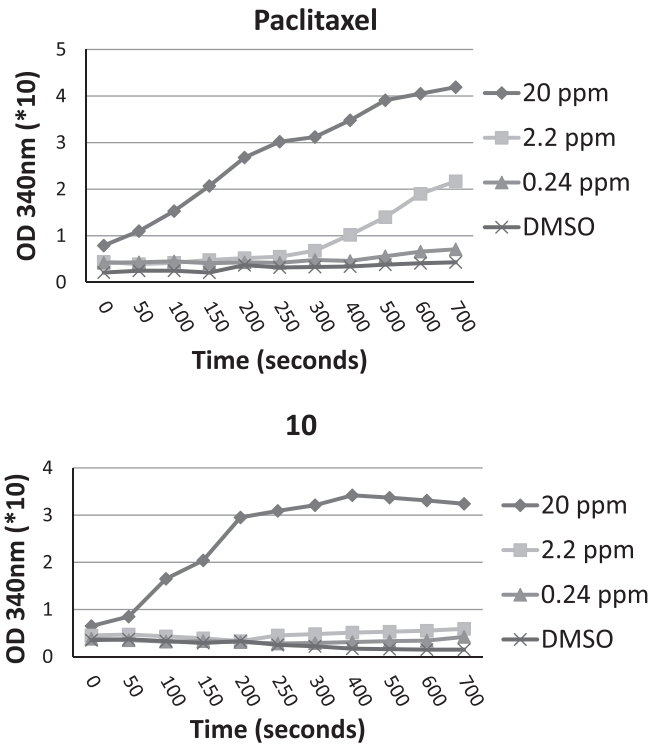

Figure 2. Degree of polymerization of pure porcine tubulin in the presence of paclitaxel and **10** at different concentrations in function of time.

2.3.1. Influence of the substituent in pyridazine position 3 on the fungicidal activity

The best activity, especially against the Ascomycetes diseases *Mycosphaerella graminicola* and *Alternaria solani*, was achieved with 3-chloropyridazines (Table 1, entry 3). The replacement of this substituent with fluorine (entry 2) or methoxy (entry 5), easily done by nucleophilic substitution reactions, leads to a significant decrease of activity. The corresponding lactame (entry 1), which is the required building block for the 3-chloropyridazine preparation, is completely inactive.

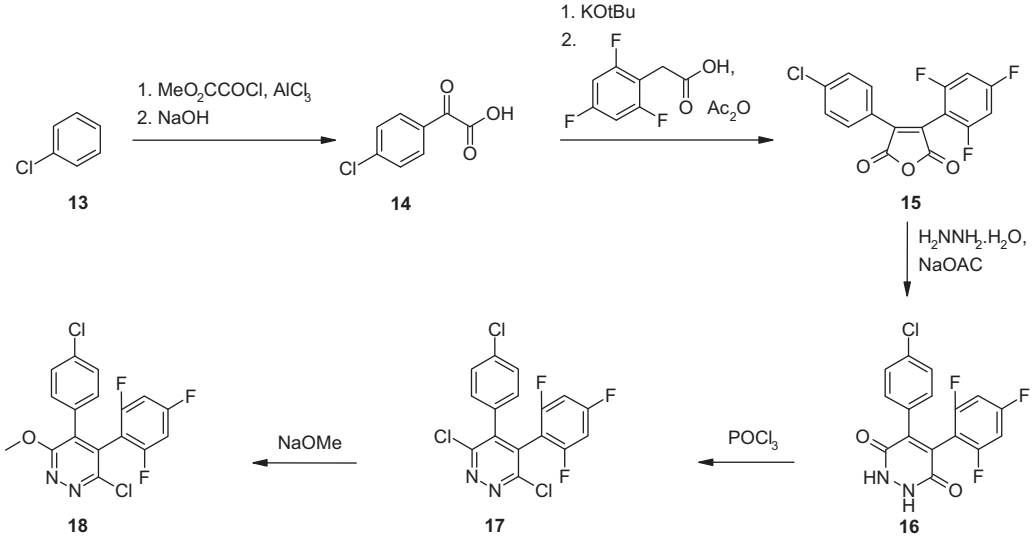

Scheme 3. Synthesis of fungicidally active pyridazines with halogen, alkoxy, alkylthio and amino substituents in position 6.

Table 1
Influence of the substituent R in pyridazine position 3 on the fungicidal activity[a]

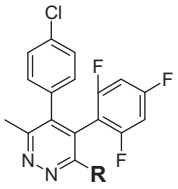

Entry	R	*Botrytis cinerea* (tomato grey mould)	*Mycosphaerella graminicola* (wheat leaf blotch)	*Alternaria solani* (tomato early blight)
1	OH	>200	>200	>200
2	F	8	191	17
3 (**4**)	Cl	6	2	2
4	CH_3	4	14	18
5	OCH_3	97	53	57

[a] Results are given as the EC_{80} (mg L^{-1}).

2.3.2. Influence of the substituent in pyridazine position 4 on the fungicidal activity

As demonstrated by the very low EC_{80} values of entry 1, pyridazines with a 2,4,6-trifluorophenyl moiety in position 4 seem to possess the highest fungicidal activity, but the replacement of the fluorine atom in the *para*-position of the phenyl ring by a methoxy group also results in excellent activity (entry 2). If one of the two *ortho*-fluorine atoms is moved to the *meta*-position of the phenyl ring (entry 3), if the *para*-methoxy group and one of the *ortho*-fluorines change places (entry 4) or if the *para*-substituent is exchanged by hydrogen (entry 5), the efficacy clearly decreases (Table 2). In principal it is possible to replace the halogenated phenyl ring in pyridazine position 4 by a similar substituted pyridine (entry 6).

Table 2
Influence of the substituent R in pyridazine position 4 on the fungicidal activity[a]

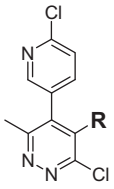

Entry	**R**	*Botrytis cinerea* (tomato grey mould)	*Mycosphaerella graminicola* (wheat leaf blotch)	*Alternaria solani* (tomato early blight)
1	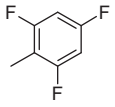	1	1	2
2	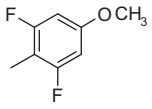	1	3	1
3	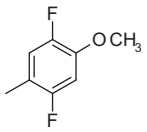	23	46	19
4	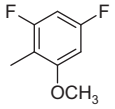	>200	95	17
5	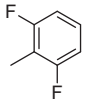	78	60	54
6	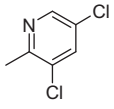	15	9	33

[a] Results are given as the EC_{80} (mg L^{-1}).

2.3.3. Influence of the substituent in pyridazine position 5 on the fungicidal activity

In principal this position of the pyridazine ring offers the greatest flexibility, because several different substituents deliver a high level of fungicidal activity (Table 3). Entries 2 and 3 demonstrate, that 2-pyridyl as well as 3-pyridyl rings linked to pyridazine position 5 offer very low EC_{80} values and therefore excellent efficacy. Another successful substituent in this position are *para*-substituted phenyl rings, here the 4-ethynyl-substituted derivative (entry 5) is clearly more active than the *para*-chlorophenyl lead compound **4** (entry 4).[38] A benzyl group linked via the methylene group to the pyridazine (entry 6) seems to possess a weaker activity than the already mentioned aryl or heteroaryl rings.

2.3.4. Influence of the substituent in pyridazine position 6 on the fungicidal activity

It seems, that 6-methyl substituted pyridazines (entry 1) possess clearly the higher fungicidal activity compared to their

Table 3
Influence of the substituent R in pyridazine position 5 on the fungicidal activity[a]

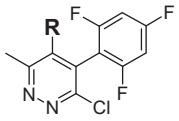

Entry	R	*Botrytis cinerea* (tomato grey mould)	*Mycosphaerella graminicola* (wheat leaf blotch)	*Alternaria solani* (tomato early blight)
1 (**10**)	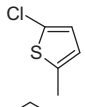	25	41	49
2	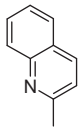	1	5	4
3	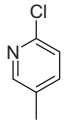	1	1	2
4 (**4**)	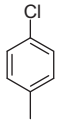	6	2	2
5	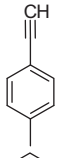	3	1	1
6		77	50	56

[a] Results are given as the EC_{80} (mg L^{-1}).

Table 4
Influence of the substituent R in pyridazine position 6 on the fungicidal activity[a]

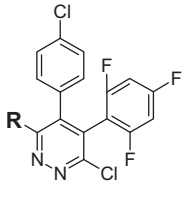

Entry	R	*Botrytis cinerea* (tomato grey mould)	*Mycosphaerella graminicola* (wheat leaf blotch)	*Alternaria solani* (tomato early blight)
1 (**4**)	CH_3	6	2	2
2 (**17**)	Cl	127	96	134
3 (**18**)	OCH_3	58	14	92
4	SCH_3	124	90	42
5	$N(CH_3)_2$	40	6	16

[a] Results are given as the EC_{80} (mg L^{-1}).

corresponding analogs with a chloro (entry 2), methoxy (entry 3), methylthio (entry 4) or a dimethylamino group (entry 5) in this position (Table 4). Only the latter mentioned amine derivative showed good activity against *M. graminicola*.

3. Conclusions

Special tetrasubstituted pyridazines are highly active against plant pathogens from the family of Ascomycetes, such as *Botrytis cinerea*, *M. graminicola* and *A. solani*, but also against several Basidiomyetes and Deuteromycetes species. Their mode of action is the promotion of tubulin polymerization, leading to the disruption of microtubule dynamics. Such special tetrasubstituted pyridazines can be prepared in only few steps, the key step is the condensation of α-unsubstituted carboxylic acids either with α-bromoketones or with α-ketoacids to five-membered ring intermediates, which subsequently are ring-enlarged with hydrazine.

A careful analysis of the structure–activity relationships enabled the identification of highly active fungicides. As it turned out, each ring carbon atom of the pyridazine scaffold has to be specifically substituted to reach the optimum efficacy. The most active pyridazine fungicides bear next to both nitrogen ring atoms a chloro atom and a methyl group. It is also important, that there is a bis-*ortho* halogen-sustituted phenyl ring with an additional *para* substituent adjacent to the chlorine. Finally, we obtained the best fungicidal results with a *para*-substituted phenyl or pyridyl moiety between the bis-*ortho* fluorophenyl ring and the methyl group.

4. Experimental section

4.1. Chemistry

All new compounds were characterized by standard spectroscopical methods. ^{1}H NMR spectra were recorded on a Varian Unity 400 spectrometer at 400 MHz using $CDCl_3$ as solvent and tetramethylsilane as internal standard. Chemical shifts are reported in ppm downfield from the standard (δ = 0.00). Mass spectra were recorded on a Micromass LCT mass spectrometer. Melting points were determined on a Büchi 535 melting point apparatus and are uncorrected. Analytical thin-layer chromatography (TLC) was performed using silica gel 60 F524 precoated plates. Preparative flash chromatography was performed using silica gel 60 (40–63 μm, E. Merck). All reactions were carried out under anhydrous conditions in an inert atmosphere (nitrogen or argon) with dry solvents.

4.1.1. 5-Chloro-thiophene-2-carboxylic acid methoxy-methyl-amide (6)

Oxalyl chloride (14.0 g, 0.11 mol) is added dropwise to a suspension of 5-chloro-thiophene-2-carboxylic acid (**5**, 15 g, 0.09 mol) and catalytic amounts of *N*,*N*-dimethylformamide in 150 ml of dichloromethane. The reaction mixture is stirred for 1 h at room temperature, then heated to reflux for 1 h. After cooling to room temperature, the reaction mixture is evaporated under reduced pressure to deliver the intermediate 5-chloro-thiophene-2-carboxylic acid chloride (16.7 g, 0.09 mol) as residue. This yellow oil was dissolved in 180 ml of dichloromethane and *N*,*O*-dimethylamine hydrochloride (9.9 g, 0.10 mol) was added at 5 °C. Subsequently triethylamine (20.5 g, 0.20 mol) was added dropwise at 5 °C. The resulting thick yellow suspension was diluted with 80 ml of dichloromethane and stirred for 16 h at room temperature. It was washed with water, the organic phase washed with brine, dried over sodium sulfate and concentrated under reduced pressure to give 5-chloro-thiophene-2-carboxylic acid methoxy-methyl-amide (**6**, 18.8 g, 0.09 mol, 98%) as a yellow oil. ^{1}H NMR ($CDCl_3$): δ = 3.38 (s, 3H), 3.80 (s, 3H), 6.96 (d, 1H), 7.79 (d, 1H). MS (ESI): *m*/*z* = 206 (M), 208 (M+2).

4.1.2. 2-Bromo-1-(5-chloro-thiophen-2-yl)-propan-1-one (7)

16 ml of a 1.5 M solution of ethylmagnesium chloride in tetrahydrofuran was added dropwise to a solution of 5-chloro-thiophene-2-carboxylic acid methoxy-methyl-amide (**6**, 6.2 g, 30 mmol) in 50 ml of tetrahydrofuran at 0 °C. The beige suspension was stirred for 2 h at the same temperature. Subsequently 25 ml of 2 N hydrochloric acid were added and the reaction mixture was poured into ethyl acetate. The organic layer was washed with brine, dried over sodium sulfate and concentrated under reduced pressure. The residue was purified by chromatography on silica gel, using ethyl acetate/heptane 1:3 as eluent, delivering 1-(5-chloro-thiophen-2-yl)-propan-1-one (4.0 g, 23 mmol) as a light yellow solid (mp 51–53 °C). This intermediate was dissolved together with 0.1 ml of a 48% solution of hydrobromic acid in glacial acetic acid in 60 ml of glacial acetic acid and cooled to 10 °C. Bromine (3.9 g, 24 mol) was added dropwise at this temperature under a nitrogen atmosphere. Subsequently the reaction mixture is stirred for 1 h at room temperature. The resulting dark red solution was concentrated under reduced pressure to deliver 2-bromo-1-(5-chloro-thiophen-2-yl)-propan-1-one (**7**, 5.8 g, 23 mmol, 77%) as a light brown oil, which could be used in the next step without further purification. ^{1}H NMR ($CDCl_3$): δ = 1.90 (d, 3H), 5.04 (q, 1H), 6.99 (d, 1H), 7.63 (d, 1H). MS (ESI): *m*/*z* = 254 (M+1).

4.1.3. 4-(5-Chloro-thiophen-2-yl)-5-hydroxy-5-methyl-3-(2,4,6-trifluoro-phenyl)-5*H*-furan-2-one (8)

Triethylamine (1.2 g, 12 mmol) was added dropwise to a solution of 2-bromo-1-(5-chloro-thiophen-2-yl)-propan-1-one (**7**, 2.9 g, 11 mmol) and 2,4,6-trifluorophenylacetic acid (2.2 g, 12 mmol) in 40 ml of acetonitrile. The reaction mixture was stirred for 16 h at room temperature, then 1,8-diazabicyclo[5,4,0]undec-7-ene (4.1 g, 27 mmol) was added slowly, keeping the temperature below 30 °C. The resulting dark brown solution was stirred 1 h at room temperature, then air was bubbled through it for 3 h, during which the colour of the solution changed to dark green. The reaction mixture was poured on saturated aqueous ammonium chloride solution and extracted with ethyl acetate. The organic layer was washed with saturated aqueous sodium bicarbonate solution and brine, dried over sodium sulfate and concentrated under reduced pressure. The residue was purified by chromatography on silica gel, using ethyl acetate/cyclohexane 1:5 as eluent, delivering 4-(5-chloro-thiophen-2-yl)-5-hydroxy-5-methyl-3-(2,4,6-trifluoro-phenyl)-5*H*-furan-2-one (**8**, 2.2 g, 6.2 mmol, 54%) as a colourless powder. Mp 155–156 °C. ^{1}H NMR ($CDCl_3$): δ = 1.93 (s, 3H), 4.51 (s, 1H), 6.74–6.89 (m, 2H), 6.93 (d, 1H), 7.42 (d, 1H). MS (ESI): *m*/*z* = 361 (M+1).

4.1.4. 5-(5-Chloro-thiophen-2-yl)-6-methyl-4-(2,4,6-trifluoro-phenyl)-2*H*-pyridazin-3-one (9)

Hydrazine hydrate (0.3 g, 9.4 mmol) was added to a solution of 4-(5-chloro-thiophen-2-yl)-5-hydroxy-5-methyl-3-(2,4,6-trifluoro-phenyl)-5*H*-furan-2-one (**8**, 2.0 g, 5.5 mmol) in 30 ml of 1-butanol. The reaction mixture was heated to 120 °C for 16 h. Upon cooling to room temperature a solid was obtained, which was filtered and washed with hexane to deliver 5-(5-chloro-thiophen-2-yl)-6-methyl-4-(2,4,6-trifluoro-phenyl)-2*H*-pyridazin-3-one (**9**, 1.3 g, 3.6 mmol, 66%) as light brown crystals. Mp 230–233 °C. ^{1}H NMR ($CDCl_3$): δ = 2.29 (s, 3H), 6.62–6.69 (m, 2H), 6.71 (d, 1H), 6.80 (d, 1H), 11.78 (br s, 1H). MS (ESI): *m*/*z* = 357 (M), 359 (M+2).

4.1.5. 3-Chloro-5-(5-chloro-thiophen-2-yl)-6-methyl-4-(2,4,6-trifluoro-phenyl)-pyridazine (10)

A suspension of 5-(5-chloro-thiophen-2-yl)-6-methyl-4-(2,4,6-trifluoro-phenyl)-2*H*-pyridazin-3-one (**9**, 890 mg, 2.5 mmol) and 5 ml of phosphorus oxychloride was heated to 110 °C for 1 h. After cooling the reaction mixture was concentrated under reduced

pressure. The remainder was taken up with ethyl acetate. The resulting solution was washed with water and brine, dried over sodium sulfate and evaporated. The residue was purified by chromatography on silica gel, using ethyl acetate/cyclohexane 1:6 as eluent, delivering 3-chloro-5-(5-chloro-thiophen-2-yl)-6-methyl-4-(2,4,6-trifluoro-phenyl)-pyridazine (**10**, 880 mg, 2.3 mmol, 94%). Mp 102–103 °C. ^{1}H NMR ($CDCl_3$): δ = 2.70 (s, 3H), 6.69–6.75 (m, 3H), 6.82 (d, 1H). MS (ESI): m/z = 375 (M), 377 (M+2).

4.1.6. 4-Chloro-phenylglyoxylic acid (14)

Methyl oxalyl chloride (265 g, 2.16 mol) was slowly added to a suspension of aluminium chloride (200 g, 1.5 mol) in 750 ml of chloroform at 0 °C. The reaction mixture was stirred for 1 h at 0 °C, then chlorobenzene (245 g, 2.19 mol) was slowly added at this temperature. The resulting mixture was stirred for 16 h at room temperature, then poured on water and diluted with dichloromethane. The phases were separated, the organic layer was washed with water, dried over sodium sulfate and evaporated. The remainder was purified by chromatography on silica gel, using ethyl acetate/heptane 1:9 as eluent, delivering methyl 4-chloro-phenylglyoxylate (99 g, 0.5 mol). This intermediate was dissolved in 800 ml of dioxane and 800 ml of 1 N sodium hydroxide were added. The mixture was stirred for 2 h at room temperature, then acidified to pH 1 with 2 N hydrochloric acid and extracted with ethyl acetate. The organic layer was washed with brine, dried over sodium sulfate and evaporated to deliver 4-chloro-phenylglyoxylic acid (**14**, 86 g, 0.47 mol 21%). ^{1}H NMR ($CDCl_3$): δ = 7.53 (d, 2H), 8.10 (br s, 1H), 8.32 (d, 2H). MS (ESI): m/z = 186 (M+1), 165 (M–OH).

4.1.7. 3-(4-Chloro-phenyl)-4-(2,4,6-trifluoro-phenyl)-furan-2,5-dione (15)

Potassium *tert*-butoxide (53 g, 0.47 mol) was added in portions to a solution of 4-chloro-phenylglyoxylic acid (**14**, 86 g, 0.47 mol) in 700 ml of methanol at room temperature. The mixture was stirred for 1 h at this temperature, then the white solid, which precipitated, was filtered, washed with cold methanol and dried in vacuo. This potassium salt was taken up in 800 ml of acetic anhydride and then 2,4,6-trifluorophenylacetic acid (73 g, 0.38 mol) was added. The reaction mixture was heated first for 1 h to 80 °C, then for 1 h to 90 °C and finally for 1 h to 100 °C. Subsequently the mixture was cooled to room temperature and the solvent was removed in vacuo to obtain 3-(4-chloro-phenyl)-4-(2,4,6-trifluoro-phenyl)-furan-2,5-dione (**15**, 148 g, 0.44 mol, 93%), which was directly used in the next step without further purification. ^{1}H NMR ($CDCl_3$): δ = 6.76–6.83 (m, 2H), 7.30 (d, 2H), 7.82 (d, 2H). MS (ESI): m/z = 339 (M+1).

4.1.8. 4-(4-Chloro-phenyl)-5-(2,4,6-trifluoro-phenyl)-1,2-dihydro-pyridazine-3,6-dione (16)

120 g of a 2:1 mixture of hydrazine hydrate and water was added dropwise to a mixture of 3-(4-chloro-phenyl)-4-(2,4,6-trifluoro-phenyl)-furan-2,5-dione (**15**, 80 g, 0.24 mol) in 270 ml of acetic acid. Sodium acetate anhydrous (22 g, 0.27 mol), was added and the reaction mixture was heated to reflux for 2 h. Subsequently the mixture was cooled, diluted with water and extracted with ethyl acetate. The organic layer was washed with brine, dried over sodium sulfate and evaporated under reduced pressure. The residue was purified by chromatography on silica gel, using ethyl acetate/heptane 1:3 as eluent, delivering 4-(4-chloro-phenyl)-5-(2,4,6-trifluoro-phenyl)-1,2-dihydropyridazine-3,6-dione (**16**, 47 g, 0.13 mol, 57%) as colourless crystals. Mp 159–164 °C. ^{1}H NMR ($CDCl_3$): δ = 6.61 (t, 2H), 7.13 (d, 2H), 7.27 (d, 2H), 11.97 (br s, 1H), 13.83 (br s, 1H). MS (ESI): m/z = 353 (M), 355 (M+2).

4.1.9. 3,6-Dichloro-4-(4-chloro-phenyl)-5-(2,4,6-trifluoro-phenyl)-pyridazine (17)

A mixture of 4-(4-chloro-phenyl)-5-(2,4,6-trifluoro-phenyl)-1,2-dihydropyridazine-3,6-dione (**16**, 45 g, 0.13 mol) and 230 ml of phosphorus oxychloride was heated to 120 °C for 2 h. The reaction mixture was cooled and evaporated under reduced pressure. The remainder was poured on water and extracted with ethyl acetate. The organic layer was washed with brine, dried over sodium sulfate and evaporated. The residue was purified by chromatography on silica gel, using ethyl acetate/heptane 1:8 as eluent, delivering 3,6-dichloro-4-(4-chloro-phenyl)-5-(2,4,6-trifluoro-phenyl)-pyridazine (**17**, 29 g, 75 mmol, 57%) as beige crystals. ^{1}H NMR ($CDCl_3$): δ = 6.59 (t, 2H), 7.01 (d, 2H), 7.26 (d, 2H). MS (ESI): m/z = 390 (M), 393 (M+3).

4.1.10. 3-Chloro-5-(4-chloro-phenyl)-6-methoxy-4-(2,4,6-trifluoro-phenyl)-pyridazine (18)

0.25 g of a 30% solution of sodium methoxide in methanol was added to a solution of 3,6-dichloro-4-(4-chloro-phenyl)-5-(2,4,6-trifluoro-phenyl)-pyridazine (**17**, 0.48 g, 1.2 mmol) in 5 ml of methanol. The reaction mixture was heated to reflux for 2 h, then cooled, diluted with water and extracted with ethyl acetate. The organic layer was washed with brine, dried over sodium sulfate and evaporated. The remainder was purified by chromatography on silica gel, using ethyl acetate/heptane 1:9 as eluent, delivering 3-chloro-5-(4-chloro-phenyl)-6-methoxy-4-(2,4,6-trifluoro-phenyl)-pyridazine (**18**, 0.43 g, 1.1 mmol, 93%) as colourless crystals. ^{1}H NMR ($CDCl_3$): δ = 4.13 (s, 3H), 6.59–6.70 (m, 2H), 7.08 (d, 2H), 7.29 (d, 2H). MS (ESI): m/z = 385 (M), 387 (M+2)

4.2. Biochemistry

4.2.1. Compounds testing on pure porcine tubulin

The HTS-tubulin polymerisation assay kit (Cytoskeleton Inc., Denver, USA) has been used following the manufacturer instruction. The standard polymerisation reaction contains 100 µl volume of 4 mg/ml tubulin in 80 mM PIPES pH 6.9, 0.5 mM EGTA, 2 mM $MgCl_2$ and 1 mM GTP. The polymerisation was started by incubation at 37 °C and followed by absorption readings at 340 nm (Spectramax). Paclitaxel and DMSO were used as positive and negative controls, respectively. 3-Chloro-5-(5-chloro-thiophen-2-yl)-6-methyl-4-(2,4,6-trifluoro-phenyl)-pyridazine (**10**) was added in different wells of a 96-well plate at the beginning of the reaction at different concentrations (20, 2.2, 0.24 ppm) in a DMSO solution (0.2 mM).

4.3. Biology

All tested compounds had a purity of at least 95%, the purification has been either performed via chromatography (see Sections 4.1.5, 4.1.9 and 4.1.10) or by crystalisation.

4.3.1. Botryotinia fuckeliana (Botrytis cinerea)/tomato (action against grey mould on tomato)

Four-week old tomato plants cv. Roter Gnom were treated in a spray chamber with the formulated test compound diluted in water. The test plants were inoculated by spraying them with a spore suspension two days after application. The inoculated test plants were incubated at 20 °C and 95% rh in a greenhouse and the percentage leaf area covered by disease was assessed when an appropriate level of disease appeared on untreated check plants (5–6 days after application).

4.3.2. *Mycosphaerella graminicola* (Septoria tritici)/wheat (action against leaf blotch on wheat)

Two-week old wheat plants cv. Riband were treated in a spray chamber with the formulated test compound diluted in water. The test plants were inoculated by spraying a spore suspension on them one day after application. After an incubation period of 1 day at 22/21 °C (day/night) and 95% rh, the inoculated test plants were kept at 22/21 °C (day/night) and 70% rh in a greenhouse. Efficacy was assessed directly when an appropriate level of disease appeared on untreated check plants (16–19 days after application).

4.3.3. *Alternaria solani*/tomato (action against early blight on tomato)

Four-week old tomato plants cv. Roter Gnom were treated in a spray chamber with the formulated test compound diluted in water. The test plants were inoculated by spraying them with a spore suspension two days after application. The inoculated test plants were incubated at 22 °C/18 °C (day/night) and 95% rh in a greenhouse and the percentage leaf area covered by disease was assessed when an appropriate level of disease appeared on untreated check plants (5–7 days after application).

References and notes

1. Part 1: Crowley, P. J.; Lamberth, C.; Müller, U.; Wendeborn, S.; Nebel, K.; Williams, J.; Sageot, O.-A.; Carter, N.; Mathie, T.; Kempf, H.-J.; Godwin, J.; Schneiter, P.; Dobler, M. R. *Pest Manag. Sci.* **2010**, *66*, 178.
2. *Microtubules*; Hyams, J., Lloyd, C. W., Eds.; Wiley-Liss: New York, 1994.
3. *Anticancer Agents from Natural Products*; Cragg, G. M., Kingston, D. G. I., Newman, D. J., Eds.; CRC Press: Boca Raton, 2005.
4. Zhou, J.; Giannakakou, P. *Curr. Med. Chem. Anticancer Agents* **2005**, *5*, 65.
5. Honore, S.; Pasquier, E.; Braguer, D. *Cell. Mol. Life Sci.* **2005**, *62*, 3039.
6. Jordan, M. A.; Wilson, L. *Nat. Rev. Cancer* **2004**, *4*, 253.
7. Li, Q.; Sham, H. L. *Expert Opin. Ther. Pat.* **2002**, *12*, 1663.
8. Jordan, M. A. *Curr. Med. Chem. Anticancer Agents* **2002**, *2*, 1.
9. Jordan, M. A.; Hadfield, J. A.; Lawrence, N. J.; McGown, A. T. *Med. Res. Rev.* **1998**, *18*, 259.
10. Young, D. H.; Slawecki, R. A. *Pestic. Biochem. Physiol.* **2001**, *69*, 100.
11. Young, D. H.; Spiewak, S. L.; Slawecki, R. A. *Pest Manag. Sci.* **2001**, *57*, 1081.
12. Uchida, M.; Robertson, R. W.; Chun, S.-J.; Kim, D.-S. *Pest Manag. Sci.* **2005**, *61*, 787.
13. Kim, D.-S.; Chun, S.-J.; Jeon, J.-J.; Lee, S.-W.; Joe, G.-H. *Pest Manag. Sci.* **2004**, *60*, 1007.
14. Hammerschlag, R. S.; Sisler, H. D. *Pestic. Biochem. Physiol.* **1972**, *2*, 123.
15. Bartels-Schooley, J.; MacNeill, B. H. *Phytopathology* **1971**, *61*, 816.
16. Allen, P. M.; Gottlieb, D. *Appl. Microbiol.* **1970**, *20*, 919.
17. Serey, R. A.; Torres, R.; Latorre, B. A. *Cienc. Inv. Agr.* **2007**, *34*, 215.
18. Pees, K.-J.; Albert, G. (Shell), European Patent Application 550113 (1993).
19. Montel, F.; Lamberth, C.; Jung, P. M. J. *Tetrahedron* **2008**, *64*, 6372.
20. Crowley, P. C.; Lamberth, C.; Müller, U.; Wendeborn, S.; Sageot, O.-A.; Williams, J.; Bartovic, A. *Tetrahedron Lett.* **2010**, *51*, 2652.
21. Morishita, H.; Manabe, A. (Sumitomo), PCT Application WO 2005/121104 (2005).
22. Lewis, R. T.; Blackaby, W. P.; Blackburn, T.; Jennings, A. S. R.; Pike, A.; Wilson, R. A.; Hallet, D. J.; Cook, S. M.; Ferris, P.; Marshall, G. R.; Reynolds, D. S.; Sheppard, W. F. A.; Smith, A. J.; Sohal, B.; Stanley, J.; Tye, S. J.; Wafford, K. A.; Atack, J. R. *J. Med. Chem.* **2006**, *49*, 2600.
23. Heinisch, G.; Kopelent-Frank, H. *Prog. Med. Chem.* **1992**, *29*, 141.
24. Heinisch, G.; Frank, H. *Prog. Med. Chem.* **1990**, *27*, 1.
25. Wu, J.; Song, B.; Hu, D.; Yang, S. *Nongyao* **2011**, *50*, 630.
26. Wu, J.; Song, B.; Hu, D.; Yang, S. *Nongyao* **2010**, *49*, 703.
27. Wu, J.; Song, B.; Hu, D.; Yang, S.; Jin, L.; Lu, Y. *Nongyao* **2008**, *47*, 625.
28. Trah, S.; Lamberth, C.; Wendeborn, S. (Syngenta), PCT Application WO 2008/049584 (2008).
29. Trah, S.; Lamberth, C.; Wendeborn, S. (Syngenta), PCT Application WO 2008/009405 (2008).
30. Trah, S.; Lamberth, C.; Wendeborn, S. (Syngenta), PCT Application WO 2008/009406 (2008).
31. Lamberth, C.; Trah, S.; Dumeunier, R. (Syngenta), PCT Application WO 2009/080314 (2009).
32. Lamberth, C.; Wendeborn, S.; Trah, S.; Dumeunier, R. (Syngenta), PCT Application WO 2008/089934 (2008).
33. Black, W. C.; Brideau, C.; Chan, C.-C.; Charleson, S.; Cromlish, W.; Gordon, R.; Grimm, E. L.; Hughes, G.; Leger, S.; Li, C.-S.; Riendeau, D.; Therien, M.; Wang, Z.; Xu, L.-J.; Prasit, P. *Bioorg. Med. Chem. Lett.* **2003**, *13*, 1195.
34. Padakanti, S.; Veeramanemi, V. R.; Pattabiraman, V. R.; Pal, M.; Yeleswarapu, K. R. *Tetrahedron Lett.* **2002**, *43*, 8715.
35. Piatak, D. M.; Dorfman, R. I.; Tibbetts, D.; Caspi, E. *J. Med. Chem.* **1964**, *7*, 590.
36. Caspi, E.; Grover, P. K.; Piatak, D. M. *Chem. Ind.* **1963**, 1495.
37. Fields, E. K.; Behrend, S. J.; Meyerson, S.; Winzenburg, M. L.; Ortega, B. R.; Hall, H. K. *J. Org. Chem.* **1990**, *55*, 5165.
38. Trah, S.; Lamberth, C. (Syngenta), PCT Application WO 2011/095461 (2011).